HHS Public Access

Author manuscript

J Neural Transm. Author manuscript; available in PMC 2016 November 01.

Published in final edited form as:

J Neural Transm. 2015 November ; 122(11): 1581–1592. doi:10.1007/s00702-015-1434-0.

Genetic markers of cholesterol transport and gray matter diffusion: A preliminary study of the *CETP* I405V polymorphism

Lauren E. Salminen[a], **Peter R. Schofield**[b,c], **Kerrie D. Pierce**[b], **Xi Luo**[d], **Yi Zhao**[d], **David H. Laidlaw**[e], **Ryan P. Cabeen**[e], **Thomas E. Conturo**[f], **Elizabeth M. Lane**[g], **Jodi M. Heaps**[h], **Jacob D. Bolzenius**[a], **Laurie M. Baker**[a], **Sarah A. Cooley**[a], **Staci Scott**[a], **Lee M. Cagle**[a], and **Robert H. Paul**[a,h]

Lauren E. Salminen: LSalminen@mail.umsl.edu

[a]University of Missouri- St. Louis, Department of Psychological Sciences, 1 University Blvd., Stadler Hall 442A, St. Louis, MO 63121, 314–277–0575, Fax: 314–516–5392

[b]Neuroscience Research Australia, Barker Street Randwick, Sydney NSW 2031, Australia

[c]School of Medical Sciences, University of New South Wales, Sydney NSW 2052, Australia

[d]Brown University, Department of Biostatistics and Center for Statistical Sciences, Providence, RI, 02912

[e]Brown University, Computer Science Department, Providence, RI, 02912

[f]Washington University School of Medicine, Mallinckrodt Institute of Radiology, 510 S. Kingshighway, St. Louis, MO 63110

[g]Vanderbilt University Medical Center, 1211 Medical Center Drive, Nashville, TN, 37232

[h]Missouri Institute of Mental Health, 4633 World Parkway Circle, Berkeley, MO 63134-3115

Abstract

Variations of the cholesteryl ester transfer protein polymorphism (*CETP* I405V/rs5882) have been associated with an increased risk for neurodegeneration, particularly when examined in conjunction with the epsilon 4 isoform of apolipoprotein E (ApoE4). Despite these identified relationships, the impact of I405V on gray matter microstructure remains unknown. The present study examined the impact of the *CETP* I405V polymorphism on gray matter integrity among 52 healthy adults between ages 51–85. Gray matter was measured bilaterally using diffusion tensor imaging (DTI) metrics of fractional anisotropy (FA), mean diffusivity (MD), axial diffusivity (AD), and radial diffusivity (RD). Participants were grouped according to a dominant statistical model (II genotype vs. IV/VV genotypes) and secondary analyses were completed to examine the interactive effects of *CETP* and ApoE4 on DTI metrics. Compared to individuals with the IV/VV genotypes, II homozygotes demonstrated significantly higher MD in bilateral temporal, parietal, and occipital gray matter. Secondary analyses revealed higher FA and AD in the left temporal lobe of IV/VV genotypes with an ApoE4 allele. Our results provide preliminary evidence that *CETP* II

Correspondence to: Lauren E. Salminen, LSalminen@mail.umsl.edu.

Disclosure Statement

There are no actual or potential conflicts of interest for any of the authors on this manuscript.

homozygosity is a predisposing risk factor for gray matter abnormalities in posterior brain regions in healthy older adults, independent of an ApoE4 allele.

Keywords

CETP; *APOE*; Gray Matter; DTI

1. Introduction

Normal aging is associated with a progressive decline in cellular processes that results in marked reductions in brain integrity (Tamnes et al. 2013). Structural brain changes typically occur along an anterior to posterior gradient, and previous studies have indicated that reductions in brain volume are most pronounced in gray matter (Raz et al. 2005; Salat et al. 2004; Tamnes et al. 2013). Despite this pattern of decline, the onset and progression of age-related atrophy is recognized as variable across individuals (Moy et al. 2011; Raz et al. 2005; Tamnes et al. 2013). This variability is likely due in part to individual differences in genetic risk, vascular integrity, and oxidative stress that alter the neurophysiology of brain microstructure (Raz et al. 2010; Resnick et al. 2003; Schmidt et al. 2011).

Evidence suggests that alterations in cholesterol homeostasis may play a role in age-related neurodegeneration (Dietschy and Turley 2001; Martin et al. 2010; Vance 2012). Localized in myelin sheaths and plasma membranes of neurons and glia, cholesterol is an important regulator of nerve conduction, synaptic plasticity, and beta-amyloid (Aβ) production (Björkhem and Meaney 2004; Martin et al. 2010). Homeostasis of brain cholesterol is largely determined through extracellular cholesterol transport of high-density lipoprotein (HDL) complexes via apolipoprotein E (ApoE), and transfer of cholesteryl esters between lipoprotein complexes via the cholesteryl ester transfer protein (CETP) (Ward et al. 2010; Yu et al. 2012). Both mechanisms of transport are critical for removal of excess cellular cholesterol and are primarily dependent on the efficiency of ApoE and CETP (Dietschy and Turley 2001; Oliveira and de Faria 2011; Wood et al. 1999).

Dysregulation of brain cholesterol metabolism increases with advanced age (Bartzokis 2004; Martin et al. 2010) and age-related changes in cholesterol homeostasis are associated with aggregated Aβ deposition and tauopathy (de Chaves and Narayanaswami 2008; Grösgen et al. 2010; Leoni et al. 2010), predominantly in cerebral blood vessels and perivascular regions of the cortex (Bartzokis 2004; Björkhem and Meaney 2004). Accumulation of Aβ and hyperphosphorylated tau causes direct damage to neuronal cell bodies and myelinated axons (de Chaves and Narayanaswami 2008), thereby facilitating gliosis and degeneration (Adalbert et al. 2007). Decreased CETP can also result in reduced clearance of oxidized lipids (Oliveira and de Faria 2011) and neuronal repair (Arias-Vásquez et al. 2007). This effect is particularly damaging in the aging brain, as age-related increases in iron deposition cause lipid oxidation in gray matter structures (Ong and Halliwell 2004; Pfefferbaum et al. 2005). Iron accumulation also promotes Aβ oligomerization in gray matter that initiates vascular dysfunction prior to neurodegeneration (Bartzokis et al. 2007; Haass and Selkoe 2007). This pathological cascade places heightened demand on cholesterol transport efficiency to prevent Aβ toxicity in the neurovascular unit (ElAli and Rivest 2013).

Cholesterol transport efficiency is partially determined by genetic expression of *APOE* and *CETP* polymorphisms (de Chaves and Narayanaswami 2008; Oliveira and de Faria 2011), and variations of these genes are believed to represent predisposing risk factors for neurodegeneration. The epsilon 4 isoform of APOE (ApoE4) is currently recognized as the single largest genetic risk factor for late-onset Alzheimer's disease (Carter 2007; Coon et al. 2007; Nagy et al. 1995), and has also been associated with brain abnormalities in non-clinical populations (Nierenberg et al. 2005; Honea et al. 2009; Heise et al. 2010). The V allele of the *CETP* I405V polymorphism (rs5882) is associated with reduced expression of CETP (Boekholdt and Thompson 2003), yet a clear "risk" allele for this polymorphism has not been defined. Previous studies have examined the relationship between I405V and gray matter and reported mixed results regarding genotypic risk and brain integrity (Oliveira and de Faria 2011). It has been suggested that the relative risk of I405V alleles may depend on dynamic interactions with ApoE4 and individual health status (Qureischie et al. 2009), and these relationships might be observed at the microstructural level.

Diffusion tensor imaging (DTI) is a non-invasive technique that provides detailed information about brain microstructure *in vivo* (Basser and Pierpaoli 1996). Directional patterns of water movement are visualized using eigenvectors of three principles axes of the diffusion ellipsoid. Axial diffusivity (AD) and radial diffusivity (RD) are derived from the eigenvectors and measure water diffusion parallel and perpendicular to axon fibers, respectively, and can therefore provide independent information regarding myelin and axonal integrity (Alexander et al. 2007; Basser and Pierpaoli 1996). The diffusion tensor can also be used to calculate scalar metrics of mean diffusivity (MD) and fractional anisotropy (FA), which measure the rate and directional restriction of diffusion within an image voxel, respectively (Alexander et al. 2007; Basser and Pierpaoli 1996). When examined in white matter, decreased FA typically corresponds to decreased AD and increased RD and MD, reflecting degeneration likely as a result of axonal loss (Bennett et al. 2010; Burzynska et al. 2010).

Although DTI is commonly used for the assessment of white matter integrity, evidence suggests that DTI can reveal age-related changes in the diffusion orientation of gray matter (Jacobs et al. 2013; Molko et al. 2001; Oreja-Guevara et al. 2005; Pfefferbaum et al. 2010). Previous research has identified longitudinal increases in gray matter diffusivity (expressed as decreased FA and increased MD) in the frontal and parietal lobes of older individuals with declining memory (Jacobs et al. 2013). By contrast, a longitudinal study of healthy older adults reported increases in both FA and MD (Pfefferbaum et al. 2010), suggesting that healthy older adults demonstrate a distinct pattern of gray matter changes that is different from those with cognitive deficits. While AD and RD have traditionally been used for the assessment of myelinated axon integrity, evidence suggests that the diffusion direction of gray matter occurs both parallel (axial) and perpendicular (radial) to the cortical surface (McNab et al. 2011; Miller et al. 2011). Thus, AD and RD in the gray matter are believed to reflect microstructural integrity of pyramidal cells that are differentially oriented throughout the cortical layers (Briggs, 2010). Examining age-related changes in gray matter microstructure may provide further insight into biological mechanisms of macrostructural gray matter atrophy that is characteristic of both normal aging and neurodegenerative

disease. Thus, DTI metrics of diffusivity and anisotropy have advantages over traditional magnetic resonance imaging (MRI) methods for the assessment of gray matter microstructure.

Research has indicated that CETP and ApoE are partially responsible for homeostasis of cholesterol and clearance of toxic iron products from gray matter (Leoni et al. 2010; Stukas et al. 2014). The *CETP* 1405V polymorphism and genetic variations of *APOE* have been identified as risk factors for dysregulated brain cholesterol and transport deficiency, which may have a significant impact on gray matter microstructure. The present study examined the impact of the *CETP* I405V polymorphism on gray matter integrity in 51 healthy older adults between the ages of 51–85. Gray matter was measured using DTI indices of MD, FA, RD, and AD. Secondary analyses evaluated the interactive effects of *CETP* and *APOE* polymorphisms on gray matter integrity in a subset of these individuals.

2.0 Methods

2.1 Participants

Data were collected from a primarily Caucasian sample of 52 older individuals enrolled in a larger ongoing study of healthy cognitive aging. Individuals were recruited from the community through local print and radio advertisements and the Research Participant Registry of the Washington University Institute of Clinical and Translational Sciences (ICTS). A trained research assistant completed all pre-enrollment screening procedures. All English-speaking individuals over the age of 50 were considered for enrollment. Exclusion criteria were based on the following: history of a medical or neurological condition capable of influencing cognition (e.g., thyroid disease, multiple sclerosis, etc.), diagnosis of any Axis I or II psychiatric condition with the exception of treated depression, history of significant head injury (defined as a loss of consciousness > 30 min.), current or past substance abuse, treatment-dependent diabetes, and contraindications for MRI (e.g., claustrophobia). A physician visually inspected all MRI scans for gross radiological abnormalities (e.g., hydrocephalus) and those with abnormal scans were excluded from the study.

The Mini Mental State Examination (MMSE) (Folstein and Folstein 1975) was used to identify individuals with possible dementia. Because our study focused on identifying genetic relationships to brain integrity in older adults, we aimed to exclude individuals who met criteria for dementia. As such, individuals who scored < 24 on the MMSE were excluded from participation.

Blood pressure was measured at three time points during a separate cognitive appointment that occurred within one month of the neuroimaging session for the majority of participants. Average systolic and diastolic blood pressure were used to objectively measure presence of hypertension. Those with hypertension (defined as systolic blood pressure ≥140 or diastolic blood pressure ≥90) were not excluded given the base rate frequencies of hypertension in older populations, but frequencies of hypertension were measured between groups to account for potential confounds.

All individuals provided informed consent prior to participation in study procedures and all were financially compensated for their time. All study procedures were approved by the local institutional review board (IRB) of the corresponding institutions.

2.2 Imaging Protocol

Neuroimaging procedures were completed using a head-only Magnetom Allegra 3T MRI at Washington University in St. Louis, MO (Siemens Healthcare, Erlangen, Germany). The 3T Allegra has powerful performance gradients with a maximum strength of 40 m/T/m in a 100 μs rise time and a slew rate of 400/T/m/s. Acquisition parameters were designed to maximize whole-brain coverage and signal-to-noise ratio (SNR), while minimizing artifact. Subject head movement was restrained through specialized foam pads and application of surgical tape across the forehead. Total scan time was less than one hour. Each scanning session began with the collection of a scout scan consisting of three orthogonal planes to confirm head positioning. The same scanner hardware and vendor operating software were used through the duration of the study to ensure quality control of the acquired data.

A T1-weighted magnetization-prepared rapid-acquisition gradient echo (MP-RAGE) sequence (Mugler and Brookeman 1990), double-echo proton-density (PD)/T2-weighted turbo spin echo (TSE) sequence, and a T2-weighted fluid-attenuated inversion-recovery (FLAIR) TSE sequence (Hajnal et al. 1992) were used to obtain whole-brain structural scans. Standard shimming was implemented to adjust for magnetic inhomogeneities.

2.3 Diffusion-Weighted Imaging (DWI) Acquisition

A customized single-shot multi-slice echo-planar tensor-encoded imaging sequence was used to acquire 31 unique diffusion gradient directions that were repeated to give a total of 62 diffusion weighted volumes. The gradients were chosen to given good q-space coverage, with 24 gradients at b = 996 s/mm^2, four gradients at b = 1,412 s/mm^2, and three gradients at b = 680 s/mm^2. Ten baseline images were acquired and interleaved in the diffusion-weighted scans to allow for improved motion-correction in later processing. Sixty-four contiguous slices were obtained per contrast with a 128 x128 matrix and field of view (FOV) of 256 × 256mm (isotropic 2.0 × 2.0 × 2.0 mm voxels). Total relaxation time was 7.82s and total echo time was 86.2ms using a full-Fourier transform. Seventy-two acquisitions were averaged across 2 repeat scans. Neuroimaging data were saved to a CD and then backed up on a custom operating system.

2.4 Diffusion Metrics

Diffusion-weighted volumes were corrected for motion and eddy-current induced artifacts through affine registration to the first b=0 volume using FSL FLIRT. The orientations of the gradient encoding directions were corrected by the rotation induced by these registrations, and brain tissue was extracted using FSL BET (brain extraction tools; Oxford Centre for Functional MRI of the Brain (FMRIB)). Diffusion tensors were fit to each voxel and volumetric maps of FA, MD, RD, and AD were computed. Freesurfer version 5.1.0 was used to segment the high-resolution T1-weighted volume, producing lobe regions-of-interest that included bilateral frontal, temporal, parietal and occipital gray matter. The T1-weighted image was then rigidly registered to the diffusion FA volume using FSL FLIRT with mutual

information. Each region was then resampled to diffusion space using this transform with nearest-neighbor interpolation, and the average values of FA, MD, RD, and AD were computed in each region.

To ensure that diffusion variability across subjects was not due to partial volume averaging within the cerebrospinal fluid (CSF), we calculated the diffusion tensor and MD from different b values in the intermediate/high range, excluding the b~0 data from the analysis. By eliminating the b~0 data in the analysis, the tensor can be calculated using DWIs in which CSF signal is suppressed. We thus made a new analysis where we computed the tensor without using the five I_0 images (i.e., using only 3 perpendicular directions with b=680, the 24 directions with b~996, and the 4 tetrahedral directions (b~1412)). The CSF effect on the resulting MD measures was reduced to negligible levels for almost all regions, based on semilog signal decay graphs (data not shown). Finally, distortion in the shape of gyri across the different diffusion weightings was not a major issue, as eddy current effects were minimal, evidenced by the lack of need to apply higher-order transformations to co-register the different diffusion-weighted images and slices in this study. Statistical analysis of the re-computed MD values revealed findings that were consistent with the results observed using the b~0 data, suggesting that CSF contamination was an unlikely cofactor in this study.

2.6 Genotyping

Genomic DNA from saliva samples was obtained using the Oragene DNA collection kit (DNA Genotek, Ottawa, Canada). Samples were shipped to Genetic Repositories Australia at Neuroscience Research Australia for processing using the Autopure LS nucleic acid purification system (QIAgen, Hilden, Germany).

The *CETP* I405V polymorphism (rs5882) and *APOE* SNPs at positions 112 (rs429358) and 158 (rs7412) of the peptide sequence (Weisgraber et al. 1981) were genotyped using the Sequenom MassArray system. *APOE* isoform genotypes were assigned as previously described (Salminen et al. 2013). The allelic frequencies of all SNPs were within Hardy-Weinberg equilibrium (rs5882, $\chi^2 = 1.32$, $df = 1$, $p = 0.25$; rs429358, $\chi^2 = 3.43$, $df = 1$, $p = 0.06$; rs7412, $\chi^2 = 2.77$, $df = 1$, $p = 0.1$).

2.7 Data Analysis

Statistical analyses for the primary aims were completed using SPSS 21. Participants were grouped according to a dominant genetic model, where individuals with at least one V allele (IV/VV genotypes) were compared to individuals with the homozygous II genotype. Demographic variables such as age, gender, race, and years of education were examined between groups using either chi square analyses or independent samples t-tests. Presence of hypertension, self-reported high cholesterol, and use of statins was also examined between groups.

A series of multivariate analyses of variance (MANOVAs) were completed to examine the isolated impact of I405V on gray matter integrity, with genetic status serving as the independent variable (II ($n = 11$) vs. IV/VV ($n = 19$)) and DTI scalar metrics serving as the

dependent variables in each MANOVA. To minimize covariance, all dependent variables were grouped by diffusion metric (e.g., FA, MD, RD, AD), and measures of lobular gray matter were additionally grouped by hemisphere. Individuals with an ApoE4 allele were excluded from this analysis.

To assess how *CETP* (II vs. IV/VV), *APOE*, and age predict FA, MD, AD and RD metrics in each lobe, multivariate and univariate regression models were applied with *CETP*, *APOE*, and age as predictors and DTI metrics as the outcome variables. To assess the interaction effects between *CETP* and *APOE*, interaction terms were added to the previous regression models. Analyses were performed separately for the left and right hemispheres. Given the small numbers associated with the outcome measures, AD, MD, and RD values were multiplied by 100,000 and FA values were multiplied by 1,000 to improve readability and avoid possible round-off errors. *T* statistics and *p* values were not affected by this approach. All secondary analyses were carried out in R (version 3.0.2).

3.0 Results

Primary Analysis-Isolated I405V

No significant group differences were observed on demographic or health variables between groups (Table 1).

A significant multivariate main effect for MD was observed in lobular gray matter of the left hemisphere (Wilks' $\Lambda = 0.654$, $F(4,25) = 3.309$, $p = 0.026$, partial $eta^2 = 0.346$) and right hemisphere (Wilks' $\Lambda = 0.688$, $F(4,25) = 2.830$, $p = 0.046$, partial $eta^2 = 0.312$). Compared to IV/VV genotypes, II genotypes demonstrated significantly higher MD in bilateral temporal, parietal, and occipital lobes, with a bilateral trend effect for higher MD in the frontal lobe (Table 2).

Bilateral trend effects were observed between groups for the multivariate outcome variable of AD (left hemisphere Wilks' $\Lambda = 0.705$, $F(4,25) = 2.611$, $p = 0.060$, partial $eta^2 = 0.295$; right hemisphere Wilks' $\Lambda = 0.709$, $F(4,25) = 2.571$, $p = 0.063$, partial $eta^2 = 0.291$). Specifically, individuals with II genotypes exhibited higher AD in gray matter of all four brain lobes compared to IV/VV genotypes, but the differences did not reach statistical significance (Table 2). A similar multivariate trend effect was observed on left hemisphere RD between groups (Wilks' $\Lambda = 0.696$, $F(4,25) = 2.732$, $p = 0.052$, partial $eta^2 = 0.304$) (Table 2).

No significant differences were observed in gray matter FA for the left (Wilks' $\Lambda = 0.836$, $F(4,25) = 1.229$, $p = 0.324$, partial $eta^2 = 0.164$) or right hemispheres (Wilks' $\Lambda = 0.895$, $F(4,25) = 0.730$, $p = 0.580$, partial $eta^2 = 0.105$) between II and IV/VV genotypes. A Sequential Bonferroni correction was applied to the univariate outcomes of MD in both MANOVAs to identify the most robust relationships between I405V and gray matter diffusion. Group differences remained statistically significant in the left occipital lobe and right parietal lobe after applying the correction (Table 3; See Supplement for adjusted cutoffs).

Secondary Analyses

Univariate regression analyses of each genotype showed that AD, MD, and RD metrics were lower in bilateral gray matter of the frontal and parietal lobes among individuals with the IV/VV genotype after including age in the regression model. The effect of *APOE* did not reach statistical significance (Table 3).

The regression analysis on *CETP*, *APOE*, and age revealed a significant interaction between *CETP* and *APOE* for FA ($p = 0.036$) and AD ($p = 0.028$) in the left temporal lobe. Among carriers of an ApoE4 allele in the IV/VV group, FA and AD in the left temporal lobe were significantly higher by 23.19×10^{-3} s/mm^2 ($t = 2.16$, $p = 0.04$) and 4.93×10^{-5} s/mm^2 ($t = 2.27$, $p = 0.03$), respectively. Among non-carriers of an ApoE4 allele, left temporal FA and AD were lower by 5.63×10^{-3} s/mm^2 ($t = -0.82$, $p = 0.41$) and 1.9×10^{-5} s/mm^2 ($t = -1.37$, $p = 0.18$), respectively, but these relationships did not reach statistical significance. No significant interactions were observed in other brain regions or between *APOE* carrier status and individuals with the II genotype of *CETP*. Subsequent analyses to control for multiple comparisons using false discovery rate (FDR) revealed no significant differences by groups.

4.0 Discussion

Results from the present study revealed distinct patterns of gray matter abnormalities among otherwise healthy older adults with genetic variations of the *CETP* I405V polymorphism. Compared to individuals with a V405 allele, II homozygotes demonstrated diffuse abnormalities in bilateral gray matter of all four brain lobes, independent of the presence of an ApoE4 allele. These effects were significant in gray matter of the left frontal and left parietal lobes after adjusting for the effects of age in the secondary analyses. Interactive relationships between *CETP* and *APOE* on DTI metrics were limited, with the exception of higher FA and AD in the left temporal lobe of IV/VV genotypes with an ApoE4 allele evidenced in the unadjusted analyses. Collectively our results indicate that the II genotype of I405V represents an independent risk factor for gray matter decline among healthy older adults. This study also provides preliminary evidence that the V405 allele may confer regional neuroprotection against gray matter damage in the presence of an ApoE4 allele.

Previous studies have reported conflicting relationships between I405V and brain integrity (Arias-Vásquez et al. 2007; Izaks et al. 2012; Murphy et al. 2012; Qureischie et al. 2009; Rodríguez et al. 2006; Sanders et al. 2010; Yu et al. 2012). Among community-dwelling older adults, VV homozygotes have been associated with a slower rate of memory decline compared to II homozygotes (Sanders et al. 2010). Izaks et al. (2012) also reported a significant interaction between V405 homozygosity, age, and increased cognitive function among a community sample of adults over the age of 65. Conversely, longitudinal studies of brain aging have associated V405 homozygosity with an increased risk for Alzheimer's disease (Arias-Vásquez et al. 2007), increased rate of cognitive decline, and higher density of neuritic plaques at autopsy compared to II homozygotes (Yu et al. 2012).

Evidence suggests that variability in the results of previous studies noted above may be due to interactions between I405V and ApoE4. Murphy et al. (2012) reported a protective effect of V405 on medial temporal lobe volume among individuals with an ApoE4 allele. Among

ApoE4 non-carriers, however, the I405 allele was protective against medial temporal lobe atrophy at baseline examination and over a one-year period (Murphy et al. 2012). This is noteworthy since the interaction observed in the present study resulted in higher FA in the left temporal lobe. Although the functional consequences of increased FA in temporal lobe gray matter has not been defined, previous research in patients with multiple sclerosis have associated increased gray matter FA with greater severity of cortical lesions and clinical impairments (Calabrese et al. 2011; Rovaris et al. 2005). Conversely, findings by Jacobs et al. (2013) revealed negative associations between decreased FA and cortical thinning in posterior gray matter regions of individuals with memory difficulties. Considering the methodological parameters of these studies, increased temporal lobe FA in IV/VV genotypes with an ApoE4 likely reflects greater integrity of gray matter microstructure. While it is currently unclear why interactive effects of *APOE* and *CETP* were specific to the temporal lobe, one possibility is that CETP activity is heightened in this brain region in order to compensate for temporal lobe beta-amyloid aggregation associated with the ApoE4 allele. This interpretation remains conjecture at this point and further research is needed to determine the clinical significance of directional changes in gray matter FA. Future studies utilizing Pittsburgh compound B (PIB) imaging are warranted to determine the potential interaction between I405V and amyloid deposition in the brain (for review see Rabinovici and Jagust 2009).

Secondary results revealed independent effects of *CETP* on MD in frontal and parietal gray matter after adjusting for the effects of age. These findings partially support work by Jacobs et al. (2013) who reported decreased FA and increased MD over a 12-year period in frontal and parietal lobe gray matter of individuals with declining memory. In contrast to results of the present study, changes in gray matter diffusivity were only observed in individuals with cognitive abnormalities (Jacobs et al. 2013). Previous research has indicated that age-related microstructural gray matter changes may be too subtle to significantly influence FA values (Castriota-Scanderbeg et al. 2003), likely due to the minimal directional restriction of water diffusion in healthy gray matter. It is possible that there is a minimum threshold of microstructural gray matter damage that is necessary to alter FA values, and this may be region-specific. If so, this would explain why previous studies have observed FA changes in specific gray matter regions among clinical populations (Jacobs et al. 2013; Molko et al. 2001; Taoka et al. 2007; Wieshmann et al. 1999), whereas no significant differences were observed among the healthy participants in the primary analysis of this study. It is possible that FA changes in frontal and parietal gray matter reflect neurodegenerative processes underlying clinical pathology, whereas MD changes in these regions reflect normal aging. Further research is needed to investigate potential mechanisms by which changes in scalar metrics occur in aging gray matter.

Genetic differences in DTI metrics were observed as simultaneous increases in gray matter MD, RD, and AD (referred to as an absolute increase in diffusivity) and relatively stable FA in non-carriers of an ApoE4 allele. Increased absolute diffusivity in gray matter is consistent with patterns of white matter decline observed in the advanced stages of Wallerian degeneration and amyotrophic lateral sclerosis (Burzynska et al. 2010; Cosottini et al. 2005; Thomalla et al. 2004). While decreased AD and increased RD could reflect initial stages of

axon fragmentation that disrupt the myelin sheath, progressive degradation of myelinated axons activates microglial phagocytosis of excess cellular debris, and a resultant increase in AD (Acosta-Cabronero et al. 2010). In this scenario, increased absolute diffusivity will occur independent of FA changes because there is a proportional change in water movement both parallel and perpendicular to the diffusion ellipsoid. Thus, phagocytic clearance of axonal fragments allows for decreased water restriction facilitating faster diffusion in all directions (Acosta-Cabronero et al. 2010). In gray matter, these changes may be a result of local tissue shrinkage, neuronal loss in juxtacortical white matter, demyelination of neurons in gyral cores and subarcuate fibers, and increased unbound interstitial fluid in the neurovascular unit (Jacobs et al. 2013; Pfefferbaum et al. 2010).

Results of the present study suggest a unique relationship between genetic variations of *CETP* and gray matter diffusion among older adults, yet the biological mechanisms by which genetic variations of the I405V polymorphism influence gray matter integrity are currently unknown. I405V is a missense polymorphism in exon 14 of the *CETP* gene that has shown to be associated with alteration of CETP function (Boekholdt and Thompson 2003; Thompson et al. 2008). In the peripheral nervous system (PNS), CETP facilitates triglyceride enrichment of densely packed LDL complexes resulting in lipid oxidation and cholesterol deposits in the sub-endothelial space of the artery wall (Havel 2000). Over time, cholesterol deposition progressively damages the vessel lumen promoting atherosclerosis, risk for occlusion, and systemic hypoperfusion (Carter 2007). Previous studies have shown that each of these factors is associated with reduced brain integrity due to alterations in blood supply that stem from pathological changes in peripheral vasculature. Cerebral changes in this context can be considered a secondary effect of chronic vessel damage in the PNS. Because lipoproteins do not readily cross the blood brain barrier (Björkhem and Meaney 2004; Vance 2012), altered CETP expression in the CNS may be an independent risk factor for structural abnormalities.

Given the limited literature investigating brain-behavior relationships with *CETP* I405V, we were unable to make an *apriori* hypothesis regarding cognitive difficulties associated with II versus IV/VV genotypes. As such, we chose to focus on genetic differences in brain integrity versus cognition, to establish preliminary relationships between region-specific differences in gray matter and *CETP* genotypes. It is important that future studies consisting of larger cell sizes investigate relationships between I405V, gray matter diffusivity, and cognition to determine the applicability of these findings in a clinical setting.

In addition, we cannot infer conclusions related to the relationship between genetic status, dyslipidemia, and concentrations of brain cholesterol as lipid panels and CSF metabolites were not measured in this study. While inclusion of such measures in future studies could provide supplementary information regarding the relationship between PNS and CNS cholesterol levels, these markers cannot elucidate the nature of cholesterol transport efficiency *in vivo*. Thus, grouping individuals according to genetic variations known to influence cholesterol transport represents a strength of our study. Examination of iron content was also beyond the scope of this study and therefore we are unable to comment on the potential influence of iron on the results presented herein. We acknowledge that localized differences in iron content may mediate relationships between I405V genotypes

and gray matter changes, and recommend using additional imaging modalities (e.g., susceptibility-weighted imaging) to measure iron content in future investigations of I405V and gray matter diffusion.

A few limitations of this study should be noted. The limited cell size of individuals within each analysis warrants caution when interpreting the external validity of our results. Caution is further warranted when interpreting the results of secondary analyses given the reduced cell sizes and the restricted relationships evidenced in the adjusted analyses. As such, the results do not provide conclusive evidence of I405V/ApoE4 interactions on gray matter integrity. Nevertheless, statistically significant group differences observed in the primary analyses yielded large effect sizes that may reflect genuine differences between genetic variations of I405V. In addition, we cannot infer conclusions related to the relationship between genetic status and concentrations of brain cholesterol as CSF metabolites were not obtained in this study. While inclusion of such measures in future studies could provide supplementary information regarding the relationship between PNS and CNS cholesterol levels, measured metabolites cannot elucidate the nature of cholesterol transport efficiency *in vivo*. Thus, grouping individuals according to genetic variations known to influence cholesterol transport represents a strength of our study. This cohort has also been the subject of other genetic analyses (Salminen et al. 2013; Salminen et al. 2014a b) and as a group these studies have not been subject to multiple testing correction. It is important that future research investigations examine larger cohorts of older individuals to confirm the results presented herein.

5. Conclusion

Results of the present study provide preliminary evidence that the II genotype of the *CETP* I405V polymorphism is associated with significant abnormalities in gray matter microstructure compared to those with a V405 allele. Importantly, the most robust group differences were observed when I405V genotypes were examined independent of an ApoE4 allele. A combined effect of IV/VV and ApoE4 on increased FA in gray matter of the left temporal lobe was observed in a subset of participants. Taken together, results of the present study demonstrate novel patterns of gray matter aging that may be attributable to genetic risk factors for dysregulated cholesterol transport. Further studies employing larger sample sizes are needed to determine the degree of interaction between I405V, ApoE4, and gray matter microstructure in a comparable sample of otherwise healthy older adults. Additional research investigating the impact of genetic variation of I405V on white matter indices will be an important next step in understanding the neural correlates of genetic risk associated with this polymorphism.

Supplementary Material

Refer to Web version on PubMed Central for supplementary material.

Acknowledgments

Study Funding: Supported by the National Institutes of Health (NIH)/National Institute of Neurological Disorders and Stroke (NINDS) grants R01 NS052470 and R01 NS039538, and NIH/National Institute of Mental Health

(NIMH) grant R21 MH090494 and the Australian National Health and Medical Research Council (NHMRC) grant 1037196. DNA extractions were performed by Genetic Repositories Australia, an Enabling Facility, which is supported by NHMRC Grant 401184. Recruitment database searches were supported in part by NIH/National Center for Research Resources (NCRR) grant UL1 TR000448. Statistical procedures were supported by the NIH grants P01AA019072, P20GM103645, P30AI042853, R01NS052470, and S10OD016366.

References

Acosta-Cabronero J, Williams GB, Pengas G, Nestor PJ. Absolute diffusivities define the landscape of white matter degeneration in Alzheimer's disease. Brain. 2010; 133(2):529–539. [PubMed: 19914928]

Adalbert R, Gilley J, Coleman MP. Aβ, tau and ApoE4 in Alzheimer's disease: The axonal connection. Trends Mol Med. 2007; 13(4):135–142. [PubMed: 17344096]

Alexander AL, Lee JE, Lazar M, Field AS. Diffusion tensor imaging of the brain. Neurotherapeutics. 2007; 4(3):316–329. [PubMed: 17599699]

Arias-Vásquez A, Isaacs A, Aulchenko YS, Hofman A, Oostra BA, Breteler M, van Duijn CM. The cholesteryl ester transfer protein (CETP) gene and the risk of Alzheimer's disease. Neurogenetics. 2007; 8(3):189–193. [PubMed: 17503098]

Bartzokis G. Age-related myelin breakdown: A developmental model of cognitive decline and Alzheimer's disease. Neurobiol Aging. 2004; 25(1):5–18. [PubMed: 14675724]

Bartzokis G, Lu PH, Mintz J. Human brain myelination and amyloid beta deposition in Alzheimer's disease. Alzheimers Dement. 2007; 3(2):122–125. [PubMed: 18596894]

Basser PJ, Pierpaoli C. Microstructural and physiological features of tissues elucidated by quantitative-diffusion-tensor MRI. J Mag Res, Ser B. 1996; 111(3):209–219.

Bennett IJ, Madden DJ, Vaidya CJ, Howard DV, Howard JH. Age - related differences in multiple measures of white matter integrity: A diffusion tensor imaging study of healthy aging. Hum Brain Mapp. 2010; 31(3):378–390. [PubMed: 19662658]

Björkhem I, Meaney S. Brain cholesterol: Long secret life behind a barrier. Arterioscl Throm Vas. 2004; 24(5):806–815.

Boekholdt SM, Thompson JF. Natural genetic variation as a tool in understanding the role of CETP in lipid levels and disease. J Lipid Res. 2003; 44(6):1080–1093. [PubMed: 12639975]

Briggs F. Organizing principles of cortical layer 6. Front Neural Circuits. 2010; 4:1–8. [PubMed: 20162034]

Burzynska AZ, Preuschhof C, Bäckman L, Nyberg L, Li SC, Lindenberger U, Heekeren HR. Age-related differences in white matter microstructure: region-specific patterns of diffusivity. Neuroimage. 2010; 49(3):2104–2112. [PubMed: 19782758]

Calabrese M, Rinaldi F, Seppi D, Favaretto A, Squarcina L, Mattisi I, et al. Cortical diffusion-tensor imaging abnormalities in multiple sclerosis: A 3-year longitudinal study. Radiology. 2011; 261(3): 891–898. [PubMed: 22031708]

Carter CJ. Convergence of genes implicated in Alzheimer's disease on the cerebral cholesterol shuttle: APP, cholesterol, lipoproteins, and atherosclerosis. Neurochem Int. 2007; 50(1):12–38. [PubMed: 16973241]

Castriota-Scanderbeg A, Fasano F, Hagberg G, Nocentini U, Filippi M, Caltagirone C. Coefficient Dav is more sensitive than fractional anisotropy in monitoring progression of irreversible tissue damage in focal nonactive multiple sclerosis lesions. AJNR. 2003; 24(4):663–670. [PubMed: 12695200]

Coon KD, Myers AJ, Craig DW, Webster JA, Pearson JV, Lince DH, et al. A high-density whole-genome association study reveals that APOE is the major susceptibility gene for sporadic late-onset Alzheimer's disease. J Clin Psychiatry. 2007; 68(4):613. [PubMed: 17474819]

Cosottini M, Giannelli M, Siciliano G, Lazzarotti G, Michelassi MC, Del Corona A. Diffusion-Tensor MR imaging of corticospinal tract in amyotrophic lateral sclerosis and progressive muscular atrophy 1. Radiology. 2005; 237(1):258–264. [PubMed: 16183935]

de Chaves EP, Narayanaswami V. Apolipoprotein E and cholesterol in aging and disease in the brain. Future Lipidol. 2008; 3(5):505–530. [PubMed: 19649144]

Dietschy JM, Turley SD. Cholesterol metabolism in the brain. Curr Opin Lipidol. 2001; 12(2):105–112. [PubMed: 11264981]

ElAli A, Rivest S. The role of ABCB1 and ABCA1 in beta-amyloid clearance at the neurovascular unit in Alzheimer's disease. Front Physio. 2013; 4

Folstein MF, Folstein SE, McHugh PR. Mini-mental state: A practical method for grading the cognitive state of patients for the clinician. J Psychiatr Res. 1975; 12:189–198. [PubMed: 1202204]

Grösgen S, Grimm MO, Frieß P, Hartmann T. Role of amyloid beta in lipid homeostasis. BBA-Mol Cell Biol L. 2010; 1801(8):966–974.

Haass C, Selkoe DJ. Soluble protein oligomers in neurodegeneration: Lessons from the Alzheimer's amyloid β-peptide. Nat Rev Mol Cell Biol. 2007; 8(2):101–112. [PubMed: 17245412]

Hajnal JV, Bryant DJ, Kasuboski L, Pattany PM, De Coene B, Lewis PD, et al. Use of fluid attenuated inversion recovery (FLAIR) pulse sequences in MRI of the brain. J Comput Assist Tomo. 1992; 16(6):841–844.

Havel RJ. Genetic underpinnings of LDL size and density: A role for hepatic lipase? Am J Clin Nutr. 2000; 71(6):1390–1391. [PubMed: 10837276]

Heise V, Filippini N, Ebmeier KP, Mackay CE. The APOE e4 allele modulates brain white matter integrity in healthy adults. Mol Psychiatry. 2010; 16(9):908–916. [PubMed: 20820167]

Honea RA, Vidoni E, Harsha A, Burns JM. Impact of APOE on the healthy aging brain: A voxel-based MRI and DTI study. J Alzheimer's Dis. 2009; 18(3):553–564. [PubMed: 19584447]

Izaks GJ, van der Knaap AM, Gansevoort RT, Navis G, Slaets JP, Dullaart RP. Cholesteryl Ester Transfer Protein (CETP) genotype and cognitive function in persons aged 35 years or older. Neurobiol Agin. 2012; 33(8):1851–e7.

Jacobs HI, van Boxtel MP, Gronenschild EH, Uylings H, Jolles J, Verhey FR. Decreased gray matter diffusivity: A potential early Alzheimer’s disease biomarker? Alzheimers Dement. 2013; 9(1):93–97. [PubMed: 22651939]

Leoni V, Solomon A, Kivipelto M. Links between ApoE, brain cholesterol metabolism, tau and amyloid beta-peptide in patients with cognitive impairment. Biochem Soc Trans. 2010; 38(4): 1021–1025. [PubMed: 20658997]

Martin M, Dotti CG, Ledesma MD. Brain cholesterol in normal and pathological aging. BBA-Mol Cell Biol L. 2010; 1801(8):934–944.

McNab JA, Polimeni JR, Wang R, Augustinack JC, Fujimoto K, Stevens A, et al. Surface based analysis of diffusion orientation for identifying architectonic domains in the in vivo human cortex. Neuroimage. 2013; 69:87–100. [PubMed: 23247190]

Miller KL, Stagg CJ, Douaud G, Jbabdi S, Smith SM, Behrens TE, et al. Diffusion imaging of whole, post-mortem human brains on a clinical MRI scanner. Neuroimage. 2011; 57(1):167–181. [PubMed: 21473920]

Molko N, Pappata S, Mangin JF, Poupon C, Vahedi K, Jobert A, et al. Diffusion tensor imaging study of subcortical gray matter in CADASIL. Stroke. 2001; 32(9):2049–2054. [PubMed: 11546896]

Moy G, Millet P, Haller S, Baudois S, De Bilbao F, Weber K, et al. Magnetic resonance imaging determinants of intraindividual variability in the elderly: Combined analysis of grey and white matter. Neuroscience. 2011; 186:88–93. [PubMed: 21515341]

Mugler JP, Brookeman JR. Three – dimensional magnetization – prepared rapid gradient – echo imaging (3D MP RAGE). Magn Reson Med. 1990; 15(1):152–157. [PubMed: 2374495]

Murphy EA, Roddey JC, McEvoy LK, Holland D, Hagler DJ Jr, Dale AM, Brewer JB. CETP polymorphisms associate with brain structure, atrophy rate, and Alzheimer’s disease risk in an APOE-dependent manner. Brain Imaging Behav. 2012; 6(1):16–26. [PubMed: 21892657]

Nagy ZS, Esiri MM, Jobst KA, Johnston C, Litchfield S, Sim E, Smith AD. Influence of the apolipoprotein E genotype on amyloid deposition and neurofibrillary tangle formation in Alzheimer's disease. Neuroscience. 1995; 69(3):57–761.

Nierenberg J, Pomara N, Hoptman MJ, Sidtis JJ, Ardekani BA, Lim KO. Abnormal white matter integrity in healthy apolipoprotein E epsilon4 carriers. Neuroreport. 2005; 16(12):1369–1372. [PubMed: 16056141]

Oliveira HC, de Faria EC. Cholesteryl ester transfer protein: the controversial relation to atherosclerosis and emerging new biological roles. IUBMB Life. 2011; 63(4):248–257. [PubMed: 21488146]

Ong WY, Halliwell B. Iron, atherosclerosis, and neurodegeneration: A key role for cholesterol in promoting iron-dependent oxidative damage? Ann N Y Acad Sci. 2004; 1012(1):51–64. [PubMed: 15105255]

Oreja-Guevara C, Rovaris M, Iannucci G, Valsasina P, Caputo D, Cavarretta R, et al. Progressive gray matter damage in patients with relapsing-remitting multiple sclerosis: A longitudinal diffusion tensor magnetic resonance imaging study. Arch Neuro. 2005; 62(4):578–584.

Persson J, Lind J, Larsson A, Ingvar M, Cruts M, Van Broeckhoven C, et al. Altered brain white matter integrity in healthy carriers of the APOE ε4 allele A risk for AD? Neurology. 2006; 66(7): 1029–1033. [PubMed: 16606914]

Pfefferbaum A, Adalsteinsson E, Rohlfing T, Sullivan EV. Diffusion tensor imaging of deep gray matter brain structures: Effects of age and iron concentration. Neurobiol Aging. 2010; 31(3):482–493. [PubMed: 18513834]

Pfefferbaum A, Adalsteinsson E, Sullivan EV. Frontal circuitry degradation marks healthy adult aging: Evidence from diffusion tensor imaging. Neuroimage. 2005; 26(3):891–899. [PubMed: 15955499]

Qureischie H, Heun R, Popp J, Jessen F, Maier W, Schmitz S, et al. Association of CETP polymorphisms with the risk of vascular dementia and white matter lesions. J Neural Transm. 2009; 116(4):467–472. [PubMed: 19184337]

Rabinovici GD, Jagust WJ. Amyloid imaging in aging and dementia: Testing the amyloid hypothesis in vivo. Behav Neurol. 2009; 21(1–2):117–128. [PubMed: 19847050]

Raz N, Ghisletta P, Rodrigue KM, Kennedy KM, Lindenberger U. Trajectories of brain aging in middle-aged and older adults: Regional and individual differences. Neuroimage. 2010; 51(2):501–511. [PubMed: 20298790]

Raz N, Lindenberger U, Rodrigue KM, Kennedy KM, Head D, Williamson A, et al. Regional brain changes in aging healthy adults: General trends, individual differences and modifiers. Cereb Cortex. 2005; 15(11):1676–1689. [PubMed: 15703252]

Resnick SM, Pham DL, Kraut MA, Zonderman AB, Davatzikos C. Longitudinal magnetic resonance imaging studies of older adults: A shrinking brain. J Neurosci. 2003; 23(8):3295–3301. [PubMed: 12716936]

Rodríguez E, Mateo I, Infante J, Llorca J, Berciano J, Combarros O. Cholesteryl ester transfer protein (CETP) polymorphism modifies the Alzheimer's disease risk associated with APOE ε4 allele. J Neurol. 2006; 253(2):181–185. [PubMed: 16096813]

Rovaris M, Gallo A, Valsasina P, Benedetti B, Caputo D, Ghezzi A, et al. Short-term accrual of gray matter pathology in patients with progressive multiple sclerosis: An in vivo study using diffusion tensor MRI. Neuroimage. 2005; 24(4):1139–1146. [PubMed: 15670691]

Salat DH, Buckner RL, Snyder AZ, Greve DN, Desikan RS, Busa E, et al. Thinning of the cerebral cortex in aging. Cereb Cortex. 2004; 14(7):721–730. [PubMed: 15054051]

Salminen LE, Schofield PR, Lane EM, Heaps JM, Pierce KD, Cabeen R, et al. Neuronal fiber bundle lengths in healthy adult carriers of the ApoE4 allele: A quantitative tractography DTI study. Brain Imaging Behav. 2013; 7(3):274–281. [PubMed: 23475756]

Salminen LE, Schofield PR, Pierce KD, Conturo TE, Tate DF, Lane EM, et al. Impact of the AGTR1 A1166C polymorphism on subcortical hyperintensities and cognition in healthy older adults. AGE. 2014b; 36(4):1–8. [PubMed: 23625154]

Salminen LE, Schofield PR, Pierce KD, Lane EM, Heaps JM, Bolzenius JD. Triallelic relationships between the serotonin transporter polymorphism and cognition among healthy older adults. Int J Neurosci. 2014a; 124(5):331–338. [PubMed: 24044728]

Sanders AE, Wang C, Katz M, Derby CA, Barzilai N, Ozelius L, Lipton RB. Association of a functional polymorphism in the cholesteryl ester transfer protein (CETP) gene with memory decline and incidence of dementia. Jama. 2010; 303(2):150–158. [PubMed: 20068209]

Schmidt R, Schmidt H, Haybaech J, Loitfelder M, Weis S, Cavaleiri M, et al. Heterogeneity in age-related white matter changes. Acta Neuropathol. 2011; 122(2):171–85. [PubMed: 21706175]

Stukas S, Robert J, Wellington CL. High-Density lipoproteins and cerebrovascular integrity in Alzheimer's disease. Cell Metab. 2014; 19(4):574–591. [PubMed: 24508505]

Tamnes CK, Walhovd KB, Dale AM, Østby Y, Grydeland H, Richardson G, et al. Brain development and aging: Overlapping and unique patterns of change. Neuroimage. 2013; 68:63–74. [PubMed: 23246860]

Taoka T, Kin T, Nakagawa H, Hirano M, Sakamoto M, Wada T, et al. Diffusivity and diffusion anisotropy of cerebellar peduncles in cases of spinocerebellar degenerative disease. Neuroimage. 2007; 37(2):387–393. [PubMed: 17583535]

Thomalla G, Glauche V, Koch MA, Beaulieu C, Weiller C, Röther J. Diffusion tensor imaging detects early Wallerian degeneration of the pyramidal tract after ischemic stroke. Neuroimage. 2004; 22(4):1767–1774. [PubMed: 15275932]

Thompson A, Di Angelantonio E, Sarwar N, Erqou S, Saleheen D, Dullaart RP, et al. Association of cholesteryl ester transfer protein genotypes with CETP mass and activity, lipid levels, and coronary risk. Jama. 2008; 299(23):2777–2788. [PubMed: 18560005]

Vance JE. Dysregulation of cholesterol balance in the brain: Contribution to neurodegenerative diseases. Dis Model Mech. 2012; 5(6):746–755. [PubMed: 23065638]

Ward MA, Bendlin BB, McLaren DG, Hess TM, Gallagher CL, Kastman EK. Low HDL cholesterol is associated with lower gray matter volume in cognitively healthy adults. FNAGI. 2010; 2(29):1–8.

Weisgraber KH, Rall SC, Mahley RW. Human E apoprotein heterogeneity. Cysteine-arginine interchanges in the amino acid sequence of the apo-E isoforms. J Biol Chem. 1981; 256(17):9077–9083. [PubMed: 7263700]

Wieshmann UC, Clark CA, Symms MR, Franconi F, Barker GJ, Shorvon SD. Reduced anisotropy of water diffusion in structural cerebral abnormalities demonstrated with diffusion tensor imaging. Magn Reson Imag. 1999; 17(9):1269–1274.

Wood WG, Schroeder F, Avdulov NA, Chochina SV, Igbavboa U. Recent advances in brain cholesterol dynamics: Transport, domains, and Alzheimer's disease. Lipids. 1999; 34(3):225–234. [PubMed: 10230715]

Yu L, Shulman JM, Chibnik L, Leurgans S, Schneider JA, De Jager PL, Bennett DA. The CETP I405V polymorphism is associated with an increased risk of Alzheimer's disease. Aging Cell. 2012; 11(2):228–233. [PubMed: 22122979]

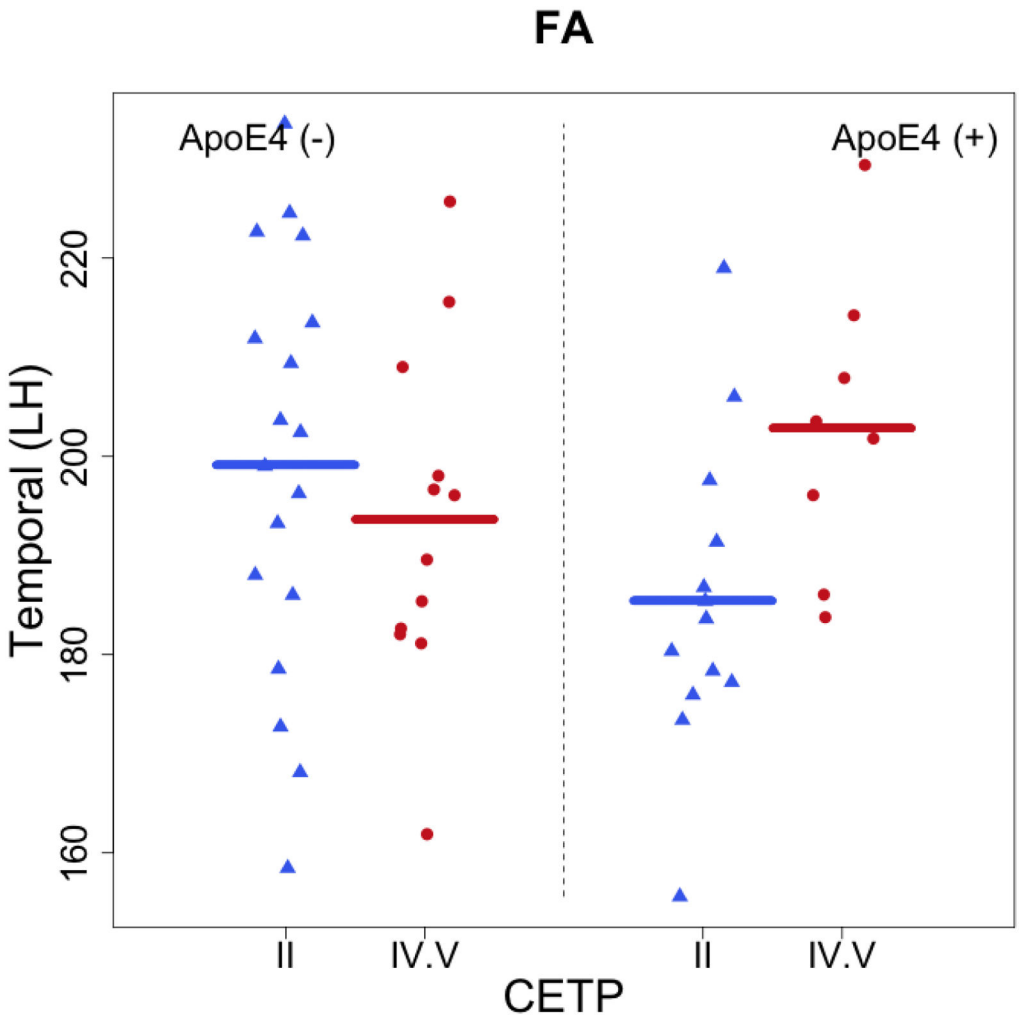

Figure 1.
Demonstrate the significant interactive effects of *CETP* and *APOE* in gray matter of the left temporal lobe. ApoE4 (+) represents individuals with at least one e4 allele, whereas ApoE4 (−) represents individuals without an e4 allele.

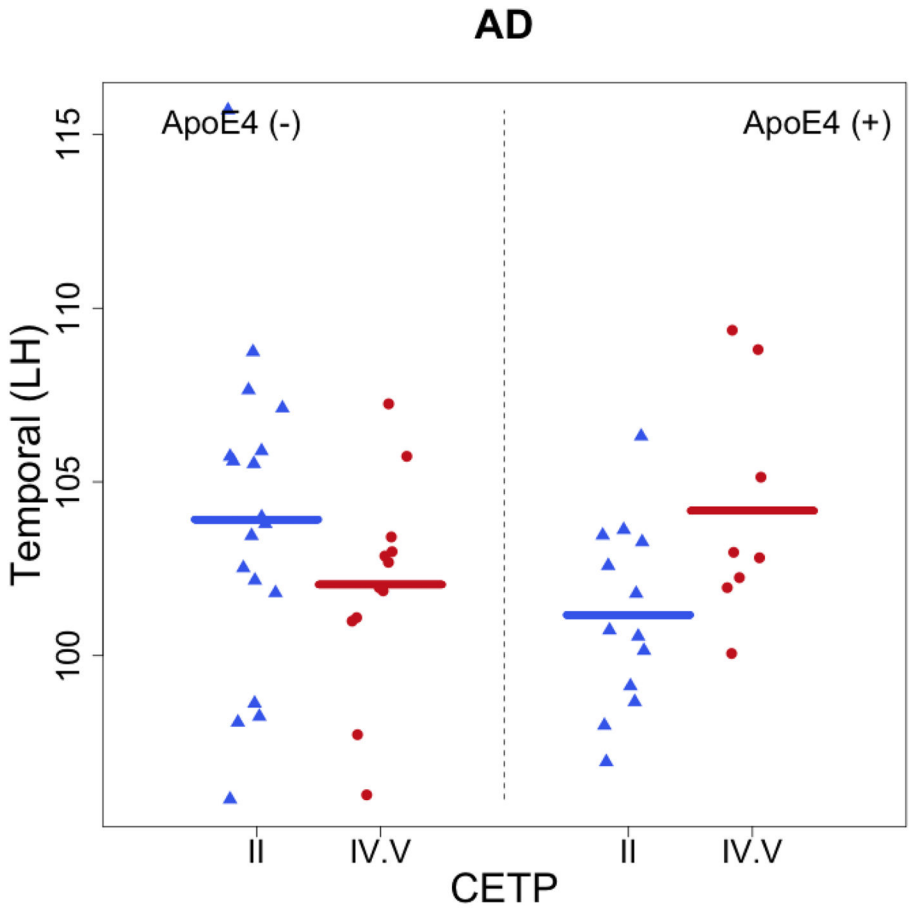

Figure 2.
Demonstrate the significant interactive effects of *CETP* and *APOE* in gray matter of the left temporal lobe. ApoE4 (+) represents individuals with at least one e4 allele, whereas ApoE4 (−) represents individuals without an e4 allele.

Table 1

Participant Characteristics

	II (*n* = 22)		IV/VV (*n* = 30)	
Genotype	**(+) ApoE4**	**(−) ApoE4**	**(+) ApoE4**	**(−) ApoE4**
Age[a]	56.64* ± 3.47	66.82 ± 9.38	61.00 ± 8.43	62.53* ± 7.58
Education, Years	15.64 ± 1.96	13.82 ± 1.83	15.30 ± 2.91	15.21 ± 2.51
Total (*n*)	11	11	11	19
Gender (*n*)[a]				
Male	2	5	3	7
Female	9	6	8	12
Race (*n*)				
Caucasian	11	9	8	12
African American	0	2	3	5
Hispanic	0	0	0	2
Hypertension[b], %	27.3	45.5	20.0	26.3
High Cholesterol[c], %	50.0	50.0	77.8	31.3
On Statins[c], %	27.3	18.2	27.3	5.3
On Antidepressants[c], %	9.1	0.0	27.3	5.3

* $p < 0.05$ Statistically significant age differences were observed between II genotypes with an ApoE4 allele and IV/VV genotypes with no ApoE4 allele.

[a] No significant differences were observed on age (p = .182) or gender (p = .643) between *CETP* groups, negative for an ApoE4 allele.

[b] Hypertension was determined by computing the average blood pressure measured across three time points. Participants were categorized as "hypertensive" based on systolic blood pressure ≥140 or diastolic blood pressure ≥90.

[c] Cholesterol was evaluated via self-report questionnaires.

Data were unavailable for seven participants. The percentage of individuals on statins and antidepressants was determined from lists of self-reported medication use provided on the demographic questionnaires.

Table 2

Relationships Between *CETP* Status and Diffusivity Metrics

Primary Analysis[a,b]	**II**	**IV/VV**			
MD	***M, SD***	***M, SD***	***F***	***p***	***partial eta***^{2}
Left Hemisphere					
Frontal	0.989 ± 0.0767	0.950 ± 0.0485	2.93	0.098	0.095
Temporal	0.901 ± 0.0523	0.859 ± 0.0351	6.95	0.013*	0.199
Parietal	0.999 ± 0.0867	0.937 ± 0.0447	6.84	0.014*	0.196
Occipital[c]	0.858 ± 0.0621	0.803 ± 0.0397	8.91	0.006*	0.241
Right Hemisphere					
Frontal	0.990 ± 0.0795	0.946 ± 0.0503	3.38	0.077	0.108
Temporal	0.912 ± 0.0650	0.868 ± 0.0457	4.43	0.044*	0.137
Parietal[c]	1.011± 0.0841	0.944 ± 0.0429	8.46	0.007*	0.232
Occipital	0.867 ± 0.0620	0.818 ± 0.0442	6.16	0.019*	0.180
AD[d]					
Left Hemisphere					
Frontal	1.13 ± 0.0814	1.09 ± 0.0491	2.67	0.114	0.087
Temporal	1.07 ± 0.0566	1.02 ± 0.0400	8.03	0.008*	0.223
Parietal	1.13 ± 0.103	1.06 ± 0.0436	6.72	0.015*	0.194
Occipital	10.0 ± 0.0983	0.94 ± 0.0380	6.22	0.019*	0.182
Right Hemisphere					
Frontal	1.13 ± 0.0835	1.09 ± 0.0526	3.47	0.073	0.110
Temporal	1.09 ± 0.0762	1.04 ± 0.0521	4.81	0.037*	0.147
Parietal	1.15 ± 0.0101	1.07 ± 0.0419	9.21	0.005*	0.248
Occipital	1.01 ± 0.0835	0.95 ± 0.0390	4.96	0.034*	0.151
RD[c]					
Left Hemisphere					
Frontal	0.919 ± 0.0748	0.880 ± 0.0485	3.04	0.092	0.098

Primary Analysis[a,b]	**II**	**IV/VV**			
MD	***M, SD***	***M, SD***	***F***	***p***	***partial eta*^{2}**
Temporal	0.816 ± 0.0357	0.778 ± 0.0357	5.56	0.026*	0.166
Parietal	0.932 ± 0.0804	0.873 ± 0.0459	6.61	0.016*	0.191
Occipital	0.786 ± 0.0503	0.734 ± 0.0418	9.19	0.005*	0.247
Right Hemisphere					
Frontal	0.917 ± 0.0777	0.875 ± 0.0495	3.30	0.080	0.105
Temporal	0.823 ± 0.0621	0.785 ± 0.0450	3.79	0.062	0.119
Parietal	0.941 ± 0.0791	0.880 ± 0.0442	7.39	0.011*	0.209
Occipital	0.793 ± 0.0497	0.751 ± 0.0475	5.31	0.029*	0.159

[a] Individuals with an ApoE4 allele were excluded from the primary analysis. II genotypes (n = 11) were compared against IV/VV genotypes (n = 19).

[b] Diffusivity was measured in non-standard units of s/mm^2 .

[c] MD in the left occipital and right parietal lobes remained significant after applying a Sequential Bonferonni correction (See Supplement for adjusted cutoffs).

[d] Results of the multivariate omnibus test for AD and RD did not reach statistical significance in either hemisphere.

Table 3

Regression outcomes for IV/VV genotypes and ApoE4 after controlling for age

Metric[a]	Lobe	Genotype	Regression Estimate	SD	*t* value	*p* value[b]
AD	Left Parietal	IV/VV	−3.684	1.737	−2.121	0.039*
		ApoE4	1.256	1.826	0.688	0.495
	Left Frontal	IV/VV	−3.236	1.446	−2.238	0.030*
		ApoE4	2.708	1.521	1.781	0.081
	Right Parietal	IV/VV	−3.794	1.807	−2.099	0.041*
		ApoE4	1.108	1.900	0.583	0.563
	Right Frontal	IV/VV	−2.948	1.513	−1.948	0.057
		ApoE4	0.335	1.591	0.211	0.834
MD	Left Parietal	IV/VV	−3.363	1.611	−2.087	0.042*
		ApoE4	1.121	1.694	0.662	0.511
	Left Frontal	IV/VV	−3.179	1.361	−2.336	0.024*
		ApoE4	2.308	1.431	1.613	0.113
	Right Parietal	IV/VV	−3.168	1.647	−1.923	0.061
		ApoE4	1.095	1.732	0.632	0.530
	Right Frontal	IV/VV	−2.768	1.418	−1.952	0.057
		ApoE4	0.285	1.491	0.191	0.849
RD	Left Parietal	IV/VV	−3.202	1.576	−2.032	0.048*
		ApoE4	1.054	1.657	0.636	0.528
	Left Frontal	IV/VV	−3.150	1.336	−2.358	0.023*
		ApoE4	2.109	1.404	1.501	0.140
	Right Parietal	IV/VV	−2.856	1.614	−1.770	0.083
		ApoE4	1.088	1.697	0.641	0.525

Metric[a]	Lobe	Genotype	Regression Estimate	SD	*t* value	*p* value[b]
	Right Frontal	IV/VV	−2.678	1.383	−1.937	0.059
		ApoE4	0.259	1.454	0.178	0.859

[a] AD, MD and RD metrics were measured in s/mm^2

[b] Additional analyses to control for the false discovery rate (FDR) revealed no significant interactions between groups. See Supplement for FDR adjusted *p* values.

$^{*}p < 0.05$